Available online at www.sciencedirect.com

SciVerse ScienceDirect

Journal of the European Ceramic Society 32 (2012) 2831–2841

www.elsevier.com/locate/jeurceramsoc

Characterization and properties of treated smectites

Aitana Tamayo [a,*], Joanna Kyziol-Komosinska [b], M[a]Jesus Sánchez [a], Pio Calejas [a], Juan Rubio [a], M[a]Flora Barba [a]

[a] *Ceramic and Glass Institute, CSIC, Madrid, Spain*
[b] *Institute of Environmental Engineering PAS, Zabrze, Poland*

Received 14 October 2011; received in revised form 22 December 2011; accepted 28 December 2011
Available online 18 January 2012

Abstract

Two natural smectite clays named BC and AC were thermal and chemically treated. Apart from smectite, quartz and kaolinite, BC clay also contains calcite, whereas illite and higher quartz content is found in AC. Treatment at 823 K leads to a collapse of the smectite structure. Treating with H_2SO_4 or NaOH also leads to the elimination of calcite and Al and Si ions. The higher swelling capacity of BC clay is in accordance with its higher cation exchange capacity.

γ_S^d values for both smectites decreases with the applied treatments. The surface acid–base constants determined for BC clay are higher than those obtained for AC independently of the applied treatment. This result together with the higher nanorugosity index, has been attributed to the higher quartz of the AC clay. Moreover, it has been observed that the cationic exchange capacity increases in both clays with the acidity of the surface.

Keywords: Clays; Surfaces; Surface energy; Traditional ceramics

1. Introduction

Clays and clay minerals have a wide and extensive variety of environmental applications, for example, as low-cost and efficient sorbents of heavy metal ions and organic compounds from water and wastewater. Also, clay barriers play a key role in the concept of long-term disposal of radioactive waste. The most commonly used clay minerals are kaolinites, illites and smectites (mainly montmorillonite and beidellite). Mixed layered clay variations also exist consisting of an arrangement of different layers of the clays from the above groups (e.g. smectite/illite)[1] or even in polymer/clay systems.[2,3] Clay minerals occur very often as fine-grained sedimentary rocks such as bentonites, shale and mudstone.

The 2:1 structure of smectites is formed by two tetrahedral sheets bonded to an octahedral layer. The tetrahedral sheets, built of T_2O_5 units, normally contain Si, Al or Fe as the central atom. Two types of octahedral sheets occur in smectites: the *dioctahedral* type, where two-thirds of the octahedral sites are occupied mainly by trivalent cations, e.g. Al(III) or Fe(III), and the *trioctahedral* type, with most of the sites occupied by divalent cations, e.g. Mg(II). The negative charge of the layers is balanced by hydrated exchangeable cations in the interlayers (mostly Ca^{2+}, Mg^{2+}, Na^{+}).[4] The structure, chemical composition, exchangeable ion type and small crystallite size of smectite clays are responsible for several of their unique properties, including large chemically active surface area, high cation exchange capacity (CEC), interlamellar surfaces with unusual hydration characteristics, and sometimes the ability to modify strongly the flow behaviour of liquids.

In spite of the layered structure, general chemical composition and size, which are typical characteristics of clay minerals, the heterogeneous character of the clays and clay minerals is strongly affected by the mineral impurities and, therefore, their surface properties will vary upon the geological environment of the clay deposit. The surface energy of a solid surface is a complex function of its components at the molecular level. The existence of several types of active sites including Brönsted and Lewis sites and ionic exchange sites provides good expectations for using clays as selective sorbents. Heterogeneities may also play an important role upon the interaction capacity of the clays with the cationic solution,

* Corresponding author at: Ceramic and Glass Institute, Kelsen 5, 28049 Madrid, Spain. Tel.: +34 91 735 58 40; fax: +34 91 735 58 43.
E-mail address: aitanath@icv.csic.es (A. Tamayo).

0955-2219/$ – see front matter © 2012 Elsevier Ltd. All rights reserved.
doi:10.1016/j.jeurceramsoc.2011.12.029

and the high-energy sites, related with the lateral surface of the clay structure, are particularly active sites for various types of interactions.[5]

It is also long known that the surface properties of clays may be also modified supplying different characteristics. Modifying, by thermal or chemical (acid or alkaline) treatments and activation with surfactants, is common in the clay-based production of adsorbents, catalysts or catalyst supports with the aim of increasing the surface area, porosity and sorption capacity of the clays. The improvement of the quality of the clay in terms of metals absorption may be carried out either by intercalation techniques or acid activation.[6,7] Treatment in acidic conditions may lead to the replacement of exchangeable cations with H^+ ions increasing the surface area and acidity of the clay. The modified forms of clays have been attracting interest for uses as adsorbents for metallic ions because of their availability and competitive price. Acid activated bentonites are mainly used for purification, bleaching and stabilization of mineral oils while treatment in basic conditions may increase the reactivity of the surface groups and consequently the overall adsorption capacity.[8,9]

In some other applications, such as powder catalysis or the ceramic industry, the clays may be heat treated up to relatively high temperatures. Dehydroxylation and dehydration processes occurring during any applied thermal treatment may lead to the collapse of the clay structure and, consequently, the interlayer spacing reduction.[10] This interlayer distance influences the dispersive component of the smectite surfaces whereas the specific interaction can be correlated with their cationic exchange capability (CEC).[11] Moreover, the amount of available acidic sites is directly related with the CEC that is defined as the equivalent amount of exchangeable cations per kilogram of smectite and depends upon the basal spacing, type and valence of the cations.

In this paper, the effects of heat (523 K and 823 K) and chemical treatments on the physical and chemical properties of two clays, smectite and mixed layer smectite/illite, are analyzed. The natural and modified materials were characterized by using X-ray diffraction (XRD), energy dispersive X-ray spectroscopy (ED-XRF) and infrared spectroscopy (FTIR). Their surface properties have been analyzed by means of cationic exchange capacity (CEC), nitrogen adsorption–desorption at 77 K and Inverse Gas Chromatography at Infinite Dilution (IGC-ID). Inverse gas chromatography and adsorption techniques have been long exploded for the characterization of the specific and dispersive components of the surface of natural fillers since conventional nitrogen or carbon dioxide adsorption characterization does not take into account the specific surface chemistry effects.[11–14] However, from our knowledge, there are no published works in which a relationship between the cationic exchange capacity of the clays and their dispersive or specific component of the surface energy has been found. Here we report on the study of two natural smectites by inverse gas chromatography evidencing the correlation between the dispersive and specific properties of the clay surface and their potential use as effective heavy metal adsorbents.

2. Experimental procedure

2.1. Materials

Two natural clays from brown coal deposits in Central Poland were studied: smectite from the Belchatow Lignite Mine (named BC clay sample) and mixed layer smectite/illite from the Adamow Lignite Mine (named AC clay sample). The air-dried, mechanically ground and homogenized samples of clays were sieved through a 0.5 mm mesh before the examinations.

2.2. Modification of clays

Heat activation and chemical (acid and alkaline) treatment were applied to both BC and AC samples. For the heat activation, the natural clay samples were placed in small ceramic crucibles and heated at 523 K and 823 K for 5 h.[15] In the treatment in acid conditions, both natural clays were heated 369 K in 16% H_2SO_4 (Merck, analysis grade) at a 1/5 (w/w) solid/solution ratio for 8 h. After 2 h, the used acid was replaced by new one to avoid precipitation of $CaSO_4$, $MgSO_4$ and $FeSO_4$ salts. The samples were then cooled, pre-washed with distilled water until receiving a negative sulfate ion test with $BaCl_2$ and finally dried at 378 K.[16,17] On the other side, for the alkaline procedure, the natural clays were treated at 368 K in 5 M NaOH (Probus) by using a 1/5 (w/w) solid/solution ratio. Afterwards, the samples were pre-washed and filtered until receiving a negative Na^+ ion test. Finally, samples were dried at 378 K.[18,19]

2.3. Methods of clay characterization

The pore size was determined by using a mercury intrusion porosimeter (Carlo Erba model 2000). The specific surface areas (SSA) were obtained from the nitrogen adsorption isotherms at 77 K and water adsorption isotherms at room temperature (Fisons, Sorptomatic 1990). In both cases the BET equation was used for the calculations.[20] The mineral content of the clay samples was determined by using X-ray diffraction (XRD, Phillips APD, Cu anode, Ni filter, $\lambda = 0.154178$ nm).

Diffraction measurements were conducted within the 2θ angle of 3–80° at the scanning rate of 0.5°. This analysis, also applied to both natural and glycolated clays,[21] allowed distinguishing the presence of smectite and illite phases in both materials. The infrared (IR) spectra of the clays were obtained on a Fourier transform infrared spectrometer (FTIR, transmittance mode, the 400–4000 cm^{-1} spectral range) by applying the KBr disc technique (0.4 mg of sample and 200 mg of KBr). The chemical composition of the clays was determined by using XRF spectroscopy (Epsylon 5 spectrometer). Free iron oxides (nonsilicate or easily reducible Fe_d) were determined by using the citrate–bicarbonate–dithionate (CBD) method. The proportion SiO_2/Al_2O_3 was computed to illustrate the changes in the chemical composition.

Cation exchange capacity (CEC) was determined in 1 M NH_4OAc at pH = 7. The pH values of the clays were measured in deionized water at the suspension ratio 1:2.5 (w/w).[21]

Table 1
Probes used to characterize the surface energy of hybrid materials. It is specified the Gutmann's acceptor (AN) and donnor (DN) numbers and their specific character.

Probe	Name	AN* (kJ mol^{-1})	DN (kJ mol^{-1})	Character
n-Pentane	C5	0	0	Neutral
n-Hexane	C6	0	0	Neutral
n-Heptane	C7	0	0	Neutral
n-Octane	C8	0	0	Neutral
n-Nonane	C9	0	0	Neutral
Cyclo octane	Cy8	0	0	Neutral
Chloroform	CL	22.6	0	Acidic
Benzene	BZ	0.71	0.42	Acidic
Acetone	AC	10.4	70.72	Amphoteric
Ethyl acetate	EA	6.24	71.14	Amphoteric
Diethyl ether	DE	5.9	80.3	Basic
Tetrahydrofuran	THF	2.1	83.7	Basic

Finally, surface energies and nanorugosity indexes of the natural and treated clays were investigated by IGC-ID. A gas chromatograph (Perkin Elmer, Autosystem) fitted with a flame ionization detector (FID) was used for the IGC-ID measurements. Chromatographic columns of 30 cm long and 2 mm of internal diameter were filled with about 1 g of smectite particles of 0.2–0.3 mm for avoiding pressure drops along the column. Columns were conditioned at 463 K overnight and the FID temperature was fixed to 523 K to avoid gas condensation. The flow rate of the carrier gas (He) was fixed to 20 cm^3 min^{-1}. FID signals were analyzed by using a GC integrator (Perkin Elmer Nelson). IGC experimental measurement temperatures were 403, 413 and 423 K.

Different organic probes (Merck, high-purity-grade) have been used for the surface physic chemical characterization. These probes are selected in accordance with their chemical interaction character with solid surfaces. Table 1 summarizes the properties of the probes considered for our purpose.

In order to acquire infinite dilution chromatography, air–probe vapour mixtures were injected manually with a 1 μl Hamilton syringe. Previously, 1 μl of the corresponding liquid was injected in a 1000 ml vessel that was closed and heated up to 100 °C. This procedure assured us that all injections contained the same quantity of each vapour probe being lower than 1×10^{-3} μl.

For all smectite samples at least four injections were made for each probe and the data taken for the calculations were the corresponding arithmetic mean of the retention time. While n-alkane probes gave symmetrical (Gaussian) peaks confirming that they were in the Henry's law region, specific probes gave asymmetric elution peaks due to the acid–base interactions with the smectite surfaces. For n-alkane probes the retention times were calculated from the maximum of the peak and the calculated error between different peaks was below 3% in all cases. On the other hand, for specific probes retention times were computed from the first moment of the peak and the calculated errors were lower than 5%.[22]

The surface analysis of clays through Inverse Gas Chromatography at Infinite Dilution (IGC-ID) has been carried out as described below.

The surface energy (γ_S) of a solid can be expressed as a sum of two components: the dispersive component (γ_S^d) which describes the London type of interactions and the specific component (γ_S^{SP}) which includes all other types of interactions (H-bonding, polar, acid–base, etc.):

$$\gamma_S = \gamma_S^d + \gamma_d^{SP} \quad (1)$$

Both γ_S^d and γ_S^{SP} surface characters can be investigated by IGC-ID taken into account that they are related to the free energy change, ΔG_A, of different non-specific and specific organic probes adsorbed on the solid surface. Then Eq. (1) can be rewritten as:

$$\Delta G_A = -\Delta G_A^d - \Delta G_A^{SP} \quad (2)$$

where ΔG_A^d and ΔG_A^{SP} are the dispersive and specific interaction contributions to ΔG_A, respectively.

The dispersive component of the surface free energy, γ_S^d, can be determined by the injection of a series of n-alkane probes into the chromatographic column packed with smectite clay particles. The slope of the n-alkane retention line gives the free energy of adsorption of a $-CH_2-$ group, $\Delta G_{A\ (-CH_2-)}^d$. Then, γ_S^d is calculated according to[23]:

$$\gamma_S^d = \frac{1}{4(\gamma_{(-CH_2-)})}\left(\frac{\Delta G_{A(-CH_2-)}}{\mathrm{Na}_{(-CH_2-)}}\right)^2 \quad (3)$$

where N is the Avogadro number, $a_{(-CH_2-)}$ is the area occupied by a methylene ($-CH_2-$) group (0.06 nm^2), and $\gamma_{(-CH_2-)}$ is the surface energy of a solid entirely made of $-CH_2-$ groups. The variation of $\gamma_{(-CH_2-)}$ with temperature is given by $\gamma_{(-CH_2-)} = 35.6 - 0.058(T - 293)$ (in mJ m^{-2} K^{-1}).

For determining the acid-base (specific) surface properties it is necessary to inject polar probes into the chromatographic column. Here, both dispersive and specific interactions are established with the solid surface, and then the adsorption free energy, ΔG_A, is defined by Eq. (2). In order to determine ΔG_A^{SP} in Eq. (2), it is necessary to eliminate the contribution of ΔG_A^d for any polar probe used. This procedure is carried out by plotting ΔG_A versus a given molecular probe property which does not depend on its specific character. This property can be expressed as $(h\nu_L)^{1/2}\alpha_L$,[24] a term that contains the molecular deformation polarizability, α_L, of the injected probes.

In this case all n-alkanes fall on a same line whereas specific probes fall at a given distance to the alkane-line. The difference in ordinates of any polar probe and the n-alkane line correspond to the specific interaction contribution and is considered as ΔG_A^{SP}.[25]

Taken into account that ΔG_A^{SP} is temperature dependent since it contains the entropic contributions (ΔS_A^{SP}), it is necessary its elimination being this carried out by plotting ΔG_A^{SP} versus T using the following Eq. (4):

$$\Delta G_A^{SP} = \Delta H_A^{SP} - T\Delta S_A^{SP} \quad (4)$$

Here, ΔH_A^{SP} is enthalpic specific energy that it is related to donor–acceptor interactions between the probe and the solid surface where neither dispersive nor entropic contributions exist. The acid (k_A) and base (k_B) characteristics of the solid surface

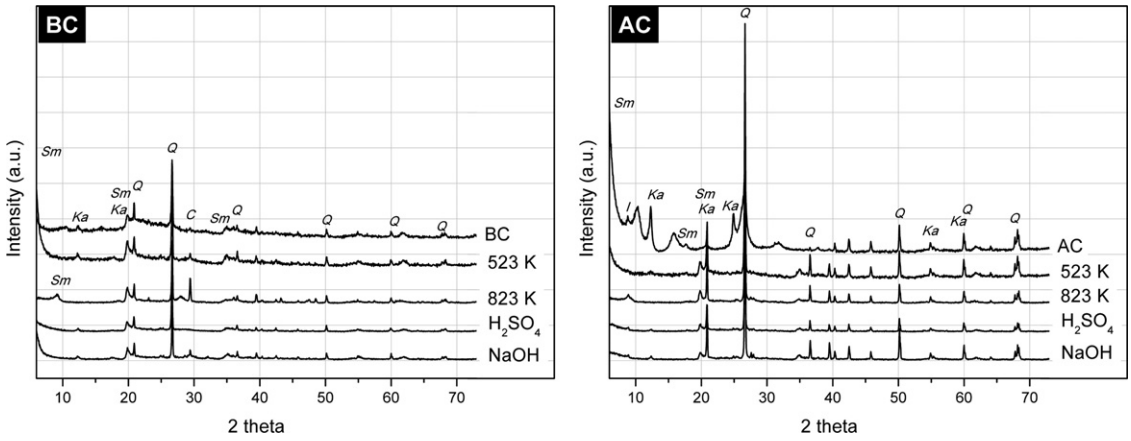

Fig. 1. XRD diffractograms of BC clay sample (left) and AC clay sample (AC) with the assignation of the main components (Sm, smectite, Ka, Kaolinite, Q, Quartz, C, Calcite).

are then obtained by Eq. (5), where it is supposed that the acidic part of the specific probe interacts with the base part of the solid surface and vice versa.[25]

$$\Delta H_A^{SP} = k_A \mathrm{DN} + k_B \mathrm{AN}^* \quad (5)$$

Here, DN and AN* are the Gutmann's donor and acceptor numbers of the probe molecules, respectively[26] modified by Riddle–Fowkes.[27]

Finally, if linear and branched alkanes are used as chromatographic probes, IGC-ID has also been proved to be useful for determining the nanomorphological index (I_M) of the solid surface.[28] Differences of surface interactions between linear and branched alkane molecules give a quantitative description of the surface accessibility of such molecules to the solid surface. Therefore, I_M informs on the solid surface morphology at the molecular scale. According to Brendlé and Papirer[28] the definition of I_M is determined by:

$$I_M = 100\frac{(\chi_{\mathrm{exp}} - \chi_T)}{\chi_T} \quad (6)$$

where the index χ_T corresponding to a branched alkane molecule represents the interaction of a hypothetical linear alkane with a given but non-integer number of C atoms that would interact with a solid surface in the same way as the branched alkane, and χ_{exp} represents the interaction of a linear alkane molecule which posses the same χ_T of a branched alkane molecule. In summary, I_M is an indication of nanorugosity.

The theory of IGC-ID for measurement of surface energy divided solids assumes that at infinite dilution the Henry's law applies and, the retention volume (Vn) of any probe is related to the variation of the standard free energy of adsorption ΔG_A as:

$$\Delta G_A = -RT \ln V_n \quad (7)$$

Then, by using the above mentioned probes listed in Table 1 and Eqs. (3)–(6), the surface energies and morphological indexes of the studied clays can be determined.

3. Results and discussion

3.1. Mineral composition and structural characterization of natural and treated clays

To calculate the mineral content, XRD diffractograms for BC and AC clays have been normalized to the intensity of the main peak of quartz present in all samples. From this preliminar result it must be concluded that the concentration of quartz mineral is lower in the BC clay sample than in the AC sample. As observed, the main mineral component of BC was smectite (beidellite) but also quartz, calcite and kaolinite are present. As we will show in Section 3.2, this result will have strong influence in the adsorption properties. On the other hand, the main mineral components of AC were smectite, illite, kaolinite and quartz (Fig. 1).

Table 2 gives the chemical analysis of natural and treated clays. SiO_2 is the main constituent of both clays followed by Al_2O_3, being the SiO2/Al2O3 ratio slightly higher in the AC sample than BC. After treatment in acid conditions, this ratio significantly increases whereas it is reduced after the caustic treatment. These results are in accordance with the XRD characterization.

Fig. 1 shows their mineral constituents, and Fig. 2 shows the corresponding FT-IR spectra.

As expected, it has been found a correlation between the chemical composition of clays obtained by XRF spectroscopy (Table 2) and the mineral containing estimated by XRD analysis (Fig. 1); silica and alumina as major constituents along with traces of calcium, magnesium and potassium oxides were also present. The Fe_2O_3 content of BC clay sample was 6.45%, being the dominating form of iron, iron bound in the silicate lattice (96% of total iron) and the rest occurred as free iron oxides. The chemical composition of AC clay sample and its related mineral one concludes that the content of silica, alumina, calcium and magnesium oxides is lower than BC. Potassium oxides were 1.49% of the total and they dominated among the interlayer cations. These differences resulted from the presence of illite with most of the sites occupied by potassium. The Fe_2O_3 content was 4.37% and, as occurred in the BC sample, the dominating

Table 2
Chemical composition of natural and pre-treated clays (all results given in %).

Samples	SiO_2	Al_2O_3	Fe_2O_3	CaO	MgO	Na_2O	K_2O	SiO_2/Al_2O_3
BC	55.81	15.25	6.45	2.82	1.74	0.042	0.566	3.66
BC 523 K	56.65	16.57	7.65	3.23	2.32	1.11	1.321	3.42
BC 823 K	57.69	17.12	9.87	5.98	3.87	3.11	4.65	3.37
BC + H_2SO_4	92.11	5.34	0.34	0.56	0.67	0.011	0.21	17.25
BC + NaOH	32.11	40.17	1.11	2.23	2.94	20.63	0.78	0.82
AC	64.70	13.65	4.37	0.99	1.37	0.109	1.49	4.74
AC 523 K	65.52	14.36	5.18	1.81	2.11	0.921	2.12	4.56
AC 823 K	66.81	15.54	6.43	2.85	2.52	1.982	3.52	4.30
AC + H_2SO_4	94.21	4.76	0.16	0.12	0.41	0.21	0.26	19.79
AC + NaOH	37.12	23.12	6.11	4.74	3.211	22.100	4.421	1.61

form of iron was iron bound in the silicate lattice (94.4% of total iron) and the rest occurred as free iron oxides.

The IR spectra of BC (Fig. 2) present several bands around 1054 and 474 cm^{-1}, attributed to the Si–O stretching vibrations of the tetrahedral layer, and two bands at 536 and 466 cm^{-1}, due to the Si–O–Al (where Al is an octahedral cation) and Si–O–Si bending vibrations, respectively. Moreover, the doublet centred around 800 cm^{-1} and the bands at 711, 873 and 1448 cm^{-1} indicate, respectively, the quartz and calcite mixtures. In the hydroxyl bending region, together with the out of plane bending of calcite, it can be distinguish the AlFeOH deformation while Al_2OH appears at 921 cm^{-1}. This partial substitution of octahedral Al by Fe is also reflected in the spectra in the weak bands located at 3567 *y* 3588 cm^{-1}, characteristic of Fe ions in the octahedral sheets.

The multiple peaks of the band at 3623 cm^{-1} corresponding to the stretching band of OH groups, indicate presence of smectite and kaolinite minerals, either with OH groups lying between the octahedral and tetrahedral layers or the outer surface of the octahedral. Moreover, the bands at 3430 and 1654 cm^{-1} are due to stretching and bending vibration, respectively, of the H–O–H water vibrations adsorbed in smectite minerals.[29]

The FTIR spectrum of AC is characteristic of illite minerals, with the bands attributed to the Si–O vibrations of the tetrahedral layer, Si–O–Al, Si–O–Si and Al_2OH. The peaks in the region at 792 cm^{-1} with the doublet at 800 and 802 cm^{-1} indicate the presence of quartz in the illite structure.

3.1.1. *Effect of temperature activation*

Heating of the clays at 523 K caused only small changes in the XRD diffractograms, being the BC peaks corresponding to the smectite structure slightly shifted towards higher values of 2θ in the heated samples. However, heating of both clays at 823 K caused the collapse of smectite, as demonstrated by the shift of the peak to about 10 Å, and the absence of the kaolinite peaks in the clay diffractograms (Fig. 1). The collapse consists in the irreversible closure of the sheets making about 80% of the mineral active surface unavailable to reagents.

The structural changes occurring due to smectite dehydration can be also detected in the FT-IR spectra of the studied samples. The elimination of water molecules is reflected in the FT-IR spectra of BC clays as a decrease of the intensity of the IR bands located at 3623 and 1654 cm^{-1} but not so clearly observed in the spectra of the heat-treated AC clay samples because of its mineral composition (Fig. 2). Moreover, dehydration of smectite in BC clay samples causes the decrease of the bands centred around 3421, 1654 and 696 cm^{-1} while this effect is observed in the bands located at 3417 and 1668 cm^{-1} for AC.

After heating the samples, the spectra show a significant decrease in the intensities of the bands at 3623 cm^{-1} for BC and at 3631 cm^{-1} for AC, as a result of the dehydroxylation of smectite, illite and kaolinite. The disappearance of the peaks at 921 cm^{-1}, for BC and, at 917 cm^{-1} for AC, indicates the destruction of the octahedral layer and decay of the kaolinite structure.

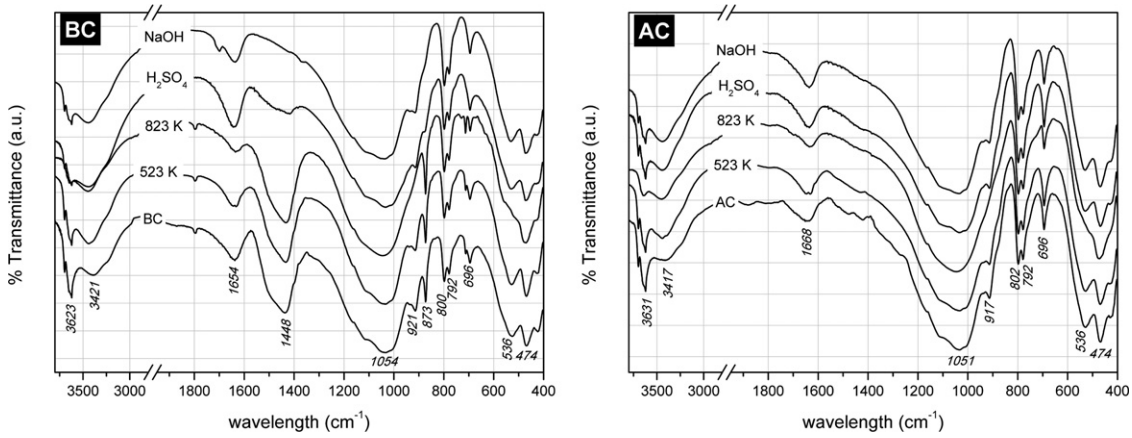

Fig. 2. FT-IR spectra of BC (left) and AC (right) clay samples.

3.1.2. Effect of acid activation

During the acid attack protons penetrate into the clay mineral layer and attack the structural OH groups. The resulting dehydroxylation is connected with the successive release of the octahedrally coordinated atoms occurring together with the elimination of the Al atoms from the tetrahedral sheets. The structural changes due to the treatment of the clays with H_2SO_4 cause the shift towards lower d-spacing with diminishing of the intensity and smoothing of the main smectite peaks in the diffractograms as an indication of the reduction in the structured areas (Fig. 1). The acid activation was more destructive to AC than to BC because AC was built of much smaller crystallites and its structure was not so well ordered as that of BC. In the XRD diffractogram of the BC clay, the peaks attributed to kaolinite remain unchanged while the calcite peak disappears. On the other hand, the modification of AC enhances the visibility of the peak corresponding to illite structure since the acid activation affects only the smectite mineral.

As an effect of dehydroxylation due to the acid treatment, the relative intensity of the band around 3421 cm^{-1} in the IR spectrum of BC clay has diminished markedly. In the acid-treated AC clay, the dehydroxilation causes the decrease of the intensity of the band centred at 3417 cm^{-1}. It is also noticed the decomposition of the octahedral layer because of the disappearance of the band centred at 873 cm^{-1} attributed to AlFeOH and the decrease in the intensity of the Al_2OH bands at 921 in BC and at 917 cm^{-1} in AC clay and the band centred at 536 cm^{-1} in both samples. The iron cations, with lower ion potential, are easier to remove since they are more weakly linked in the smectite structure than the aluminium cations, which possess high ion potential and creates therefore the strongest bonds with oxygen and OH groups. Also, it is observed the decrease in the intensity of the vibrations centred at 1054 and 1051 cm^{-1} in BC and AC clays, respectively, and the band at 474 cm^{-1} due to degradation of the tetrahedral layers. No evidence of the formation of $CaSO_4$ from precipitating is observed since it has been prevented during acid treatment by replacing at certain time the used H_2SO_4 for a new one. These results are comparable with the previously reported experiments in bentonites in which it has been stated that the acid activation of the clays leads to the dissolution of Ca^{2+}, Na^{+}, Mg^{2+}, Fe^{2+} and Fe^{3+} when present, being the Al^{3+} the more retained cations, whereas K^{+}, and Si^{4+} cations are not removed during the treatment in acidic conditions.[30]

3.1.3. Effect of alkaline activation

The XRD diffractograms reflected similarity of the effects of the alkaline and acid activations. However, the softening and lowering of the smectite peak was more evident for the AC clay sample (Fig. 1).

In the FTIR spectra, the intensity of bands at 1054 and 476 cm^{-1} for BC clay and at 1051 and 474 cm^{-1} for AC clay due to vibrations of the Si–O–Si groups in the tetrahedral layer, dropped (Fig. 2). In BC, the calcite band (1448 cm^{-1}) disappeared. Calcite was decomposed in the reaction $CaCO_3 + 2NaOH \rightarrow Na_2CO_3 + CaO\downarrow + H_2O$.

3.2. Surface area and adsorption properties of natural and treated clays

Table 3 gives the surface properties of natural and treated clays. Here it is observed that both natural clays present similar nitrogen SSA, pore sizes and porosities, but high differences appear when water SSA and CEC values are compared. This result is also valid for treated samples although major discrepancies appear for the BC clay. These results must be attributed to the different mineral and chemical constituents of both samples.

Normally, SSA calculated form water-adsorption isotherms are higher than those found by nitrogen adsorption. This general fact is due to the swelling character that presents the lattice of the clay minerals. The ratio R of water vapour to nitrogen surface areas for both clay samples indicate the marked differences existing in the mineralogical and chemical compositions of the studied clays.[31] This ratio, R, is also given in Table 3. It is clear that R increases with CEC, indicating that the clay with the higher swelling degree presents the higher CEC. At the same time, BC clay presents lower concentration of quartz than AC (Table 2), and the former one does not contains illite while AC clay does (Fig. 1). Therefore, it is clear that the minerals and their contents influence in CEC results, but the depopulation of the octahedral layers described in Section 3.1.2 seems to make a significant contribution to the catalytic activity and CEC of chemically activated smectites.[32]

Heating the studied clays at 523 K causes the water release from the smectite structure as shown in the FT-IR spectra of Fig. 2. The dehydration increases the nitrogen SSA of BC and AC clays from 41.38 to 70.94 m^2/g and from 45.56 to 53.52 m^2/g, respectively, while the water SSA increases from 141.83 to 150.20 m^2/g in BC clay and from 70.47 to 77.56 m^2/g in the AC clay sample. These results are also reproduced in the determination of the porosity by means of mercury intrusion porosimetry, leading in an increase of the % porosity after dehydration in both samples. However, the effects of this low-temperature heating of clay samples are not so evident when compared the chemical composition (Table 2) and CEC (Table 3) of both heated and non-heated samples. The reversible dehydration process upon heating clays at mild temperature has been observed in other layered materials such as bentonites in which the surface area, cristallinity and porosity changes irreversibly after heating at higher temperature.[33]

Further heating of the samples, when BC and AC clays are treated at 823 K, nitrogen and water SSA show an important decrease due to the irreversible collapse of the smectite structure. Porosity increases by 150% for BC and 390% for AC, the acidity increases up to pH lower than 7, and the CEC reaches its lowest value experimenting a decrease of ca. 25%, respect to the initial value. Moreover, from Table 2 it is clear that the chemical composition was not significantly changed, indicating that the heating treatment effects mainly occurs in the surface properties of both clays.

After acid activation, the porosity increase is marked in both samples. The nitrogen SSA increases up to 64% in AC and 87% in BC, while water SSA do not experiment a significant change (Table 3). The saturation of the sorption complex with H^{+} caused

Table 3
Properties obtained from textural characterization (where SSA is the specific surface area from nitrogen adsorption and R the water to nitrogen surface area ratio), Cationic Exchange Capacity (CEC) and clay surface acidity.

Sample	SSA (m^2/g)		R (Se_{H2O}/Se_{N2})	Pore size (μm)	Porosity (%)	CEC ($cmol_{(+)}$/kg)	pH
	N_2	H_2O					
BC	41.38	141.83	3.43	0.018	1.28	82.39	7.85
BC 523	70.94	150.20	2.12	0.032	5.32	80.4	7.83
BC 823	32.76	32.49	0.99	6.055	6.89	62.8	6.98
BC + H_2SO_4	77.44	143.21	1.85	2.107	40.11	78.55	3.39
BC + NaOH	50.09	214.09	4.27	0.636	48.21	96.57	10.28
AC	45.56	70.47	1.55	0.023	2.11	31.58	7.53
AC 523	53.52	77.56	1.45	0.038	9.23	29.05	7.67
AC 823	20.37	20.97	1.03	6.755	18.72	24.1	6.88
AC + H_2SO_4	74.83	77.98	1.04	2.764	55.12	27.98	3.29
AC + NaOH	47.07	50.92	1.08	0.901	40.07	27.39	9.95

a pH drop to about 3.5 and a decrease of CEC reaching the value of 78.55 $cmol_{(+)}$/kg and 27.98 $cmol_{(+)}$/kg for BC and AC, respectively. Regarding the chemical composition (Table 2), the proportion of silica to aluminium oxide content grows to 17.25 and 19.79, for BC and AC, respectively. The rise in percentage of silica content observed in both clay samples is attributed to the effect of acid leaching and dissolution of octahedral layers.

Finally, the alkaline treatment gives an increase in porosity of 48% and 52% for AC and BC clays, respectively. Nitrogen and water SSA increase for BC clay and remains practically invariable for AC clay due to the presence of illite and quartz in the sample. The measured pH reaches a value of 10.28 for BC and 9.95 for AC. Besides, it is also observed the dissolving of the tetrahedral layers and free silica as well, as extracted from the results presented in Table 2, where it is observed a decrease in the concentration of SiO_2 and in the silica to aluminium oxide content ratio.

3.3. Surface energy properties of natural and treated clays

The surface energy properties of the studied clays have been analyzed by means of IGC-ID. First, the dispersive surface energies and morphological indexes have been determined for both clays by injecting into the chromatographic column a series of n-alkane probes and, after that, the retention time of the polar probes allows the calculation of the specific or acid–base surface properties.

Fig. 3 shows the variation of ΔG_A as a function of the carbon number of the n-alkane chain for both natural clays. Fig. 4 shows the corresponding plot for treated clays. In all cases straight lines are obtained with regression coefficients of 0.999. γ_S^d values are obtained from the slopes of these lines by using Eq. (1) and they are given in Table 4 at the three experimental measurement temperatures.

From these data it is clear that γ_S^d decreases with the measurement temperature. The same trend has been observed in different works when studying montmorillonite samples.[34] In Table 4 it is observed that both natural clays present high dispersive surface energies, similarly to the results found for different clay materials.[12,14,34] This high surface energy is due to the partial insertion of the n-alkane molecules into structural defects existing on the border layers of the clays.[14]

The effect of the heat treatment temperature also shows a similar variation for BC and AC clays. Differences between both heat-treated smectites are more clearly observed as increases the IGC measurement temperature. This is due to the effect of high surface energy sites existing in such clays which lead to high surface energy values. At high measurement temperatures the effect of such high energy sites are minimized and differences between surface energies are better distinguishable.[35] For both BC and AC smectites, heat treated at 525 and 823 °C, the

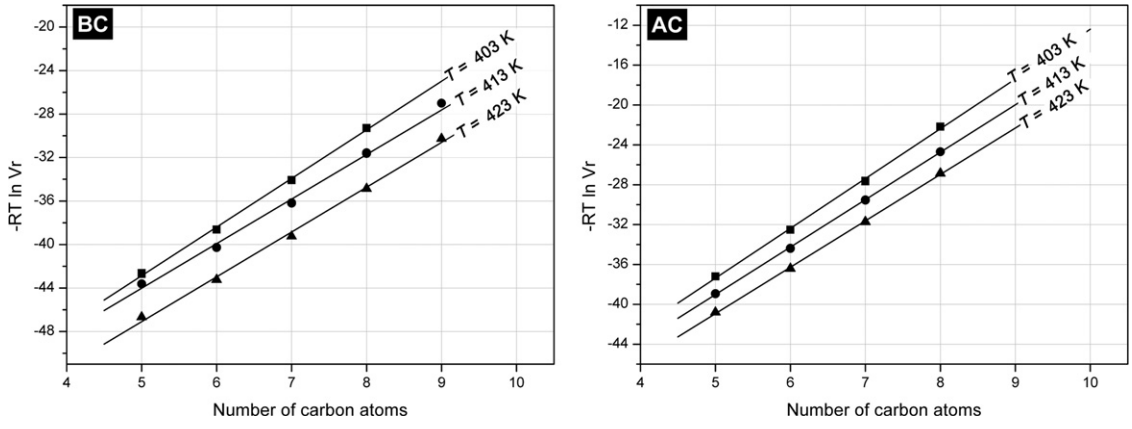

Fig. 3. Plots of –RTLn(Vn) versus carbon number for BC (left) and AC (right) natural clays.

Table 4
Surface properties of natural and treated clays. The correlation coefficient, r, of the fitting curves is also reported.

	γ_S^d			$r(\gamma_S^d)$	k_A	k_B	$r(k_A,k_B)$	I_M
	$T=403$ K	$T=413$ K	$T=423$ K					
BC	128.15	119.53	110.91	0.998	5.33	3.26	0.92	−23.18
BC 523	128.51	119.09	109.67	0.997	4.62	1.42	0.94	−12.57
BC 823	125.51	114.51	103.96	0.997	6.15	1.36	0.94	−7.18
BC H_2SO4	120.45	111.57	102.69	0.998	2.86	2.59	0.96	−9.69
BC NaOH	124.63	117.51	108.64	0.997	5.30	1.56	0.97	−15.86
AC	118.29	111.38	103.50	0.999	3.59	1.43	0.96	−11.52
AC 523	103.15	92.00	85.73	0.998	1.83	1.38	0.92	−10.15
AC 823	100.82	89.46	72.18	0.999	4.40	2.08	0.93	−6.30
AC H_2SO4	97.77	93.25	70.96	0.989	2.58	0.81	0.98	−10.36
AC NaOH	123.47	112.15	99.83	0.998	4.69	1.33	0.95	−11.31

calculation of γ_S^d values results in a decrease of the dispersive surface energy when increasing the heating temperature. This decrease is more marked in the AC clay sample than in BC. These results correspond to the reduction of the interlayer distances and microstructural modification as observed by XRD and FT-IR analysis (Figs. 1 and 2). Heat-treated clays present similar evolution of γ_S^d values with temperature to bentonite,[36] modified silicas[37] and lamellar silicas.[38]

The acid and base treatments produce different variations in γ_S^d values but both samples present similar behaviour. Table 4 shows that while H_2SO_4 treatment gives a decrease in γ_S^d, for the NaOH treated samples γ_S^d is very close the non-treated clays. Either the destruction of the smectite structure due to the H_2SO_4 treatment and the elimination of most part of the aluminium atoms have been observed to produce the determined decrease in the surface energy.[36] However, a small variation in γ_S^d values after NaOH treatment occurs in spite of the fact that the smectite structure has been highly modified as it has been discussed by XRD and FT-IR results (Figs. 1 and 2). Taken into account that after NaOH treatment the SiO_2/Al_2O_3 ratio presents a high decrease, the slight γ_S^d variation must be associated to the dissolution of quartz form the clay sample and the decomposition of the calcite into calcium oxide.

The attempts to determine the correlation between CEC and any clay surface property such as SSA, R, pore size, porosity or γ_S^d (Tables 3 and 4) concluded that, in any case normal curve fittings can be achieved. Just as illite and kaolinite clays this result indicates that no significant correlation exists.[14] Therefore, further characterization is oriented on the analysis of the acid–base properties of the clay surface. As it was detailed before, contrary to the AC clay sample, the BC clay does not contain illite and the lowest quartz concentration therefore, different acid–base behaviour should be expected. Moreover, the R value, related with the nitrogen and water adsorption isotherms, presents the larger variations along the processes, being in any case higher than 1 due to its higher swelling property.

The presence of acid and base active sites on the clay surface increases the possibility of specific intermolecular interactions with any compound. Then such interactions could be related with CEC values. Fig. 5 shows the variation of ΔG_A for both dispersive and specific probes as a function of a given probe property. Here it is observed that non-specific n-alkane molecules fall in a straight line because they only interchange dispersive interactions with the clay surface. However, specific probes are separated from the n-alkane line due to the presence of specific interactions. The specific surface energy, ΔG_A^{SP}, for any specific probe has then been obtained by Eq. (2), and afterwards Eq. (4) has been used for calculating ΔH_A^{SP} through linear fittings. These values are used for obtaining the acid and base properties (k_A, k_B) of the clay surface by using Eq. (5) as it is presented in Fig. 6. It must be taken into account that benzene gave ΔH_A^{SP} values that cannot be well-fitted with the rest

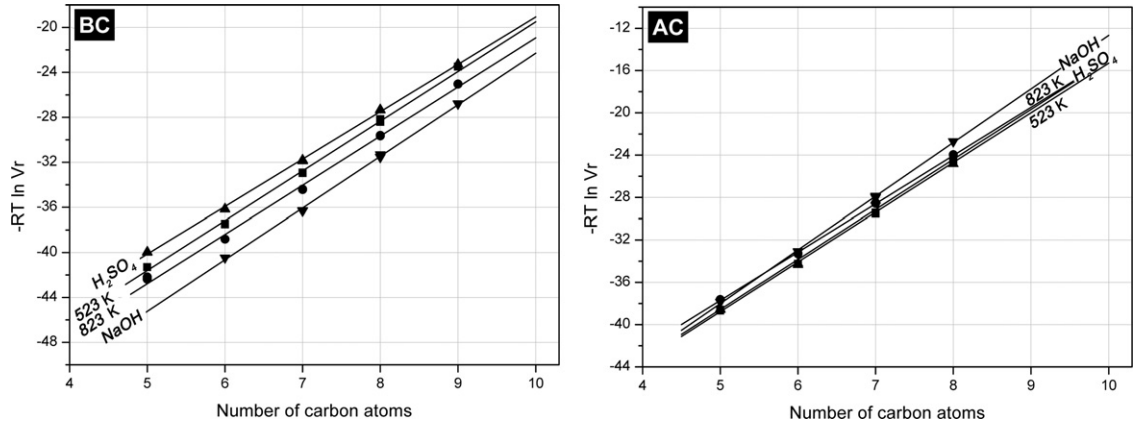

Fig. 4. Plots of –RTLn(Vn) versus carbon number for BC and AC treated clays.

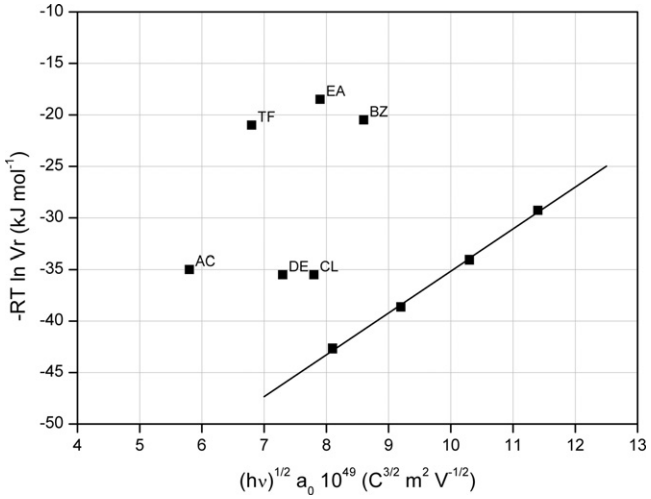

Fig. 5. Variation of ΔG_A of all studied probes as function of $[(h\nu)^{1/2}\ \alpha_0]$ for the BC clay at 423 K. ΔG_A^{SP} is calculated from the deviation of the injected polar probes from the straight line drawn for non-polar probes.

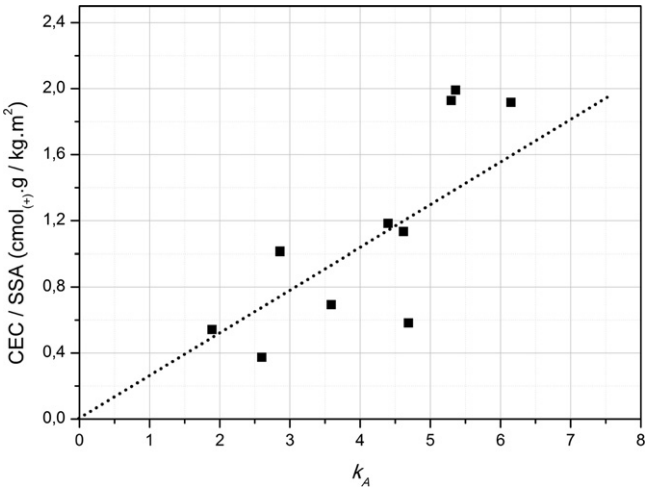

Fig. 7. Variation of CEC with k_A constant. Dotted line is plotted to guide the eye.

of the probes. A similar result has been observed for benzene when used for characterizing molecular sieve zeolites, being this fact tentatively attributed to the interaction of the benzene molecules with both kinds of adsorption sites, i.e. acid or base Lewis sites.[39,40] By using the rest of the probes linear fittings gave correlation coefficients higher than 0.92 in all cases. The obtained k_A and k_B values are collected in Table 4.

This Table 4 shows that all studied samples present meaningful k_A and k_B values, a result that indicates the presence of both Lewis acid and base surface sites in such montmorillonites. Therefore the surface of these materials can be considered as amphoteric. k_A and k_B values for natural and treated clay samples are found to be slightly higher to those reported by Cordeiro et al.[12] and Bilgiç et al.[41] for natural montmorillonite clays. Similarly to Bilgiç et al.[41] the acidity constant acquires a higher value than the basicity constant independently of the type of treatment carried out. These results indicate that the surfaces of such natural and treated montmorillonites present Lewis acid character. k_A and k_B values for natural BC clay are higher than those of AC one, a result that could be due to the presence of quartz in the AC sample. This result is also maintained for the rest of the treatments carried out in both montmorillonites.

Results of Table 4 also indicate that whatever the treatment applied in both samples, k_A and k_B values show the same trend. Thus, at 523 K both constants decrease and at 823 K they experiment an increase in their respective values, moreover the chemical treatment with H_2SO_4 leads to the higher decrease in the k_A and k_B values, but when treating with NaOH they reach similar values to those of natural samples. IGC experimental results indicate that the surface character of these samples is mainly directed by the presence of all the minerals existing in their compositions.

The successful attempt to correlate k_A and k_B with CEC gives as a result an increase of CEC with k_A as is presented in Fig. 7. In this plot we have used a reduced CEC value by dividing the measured CEC by the corresponding SSA values, i.e. CEC/SSA. This procedure has been used in order to eliminate the effect of the different surface area of both samples. Then, when CEC/SSA

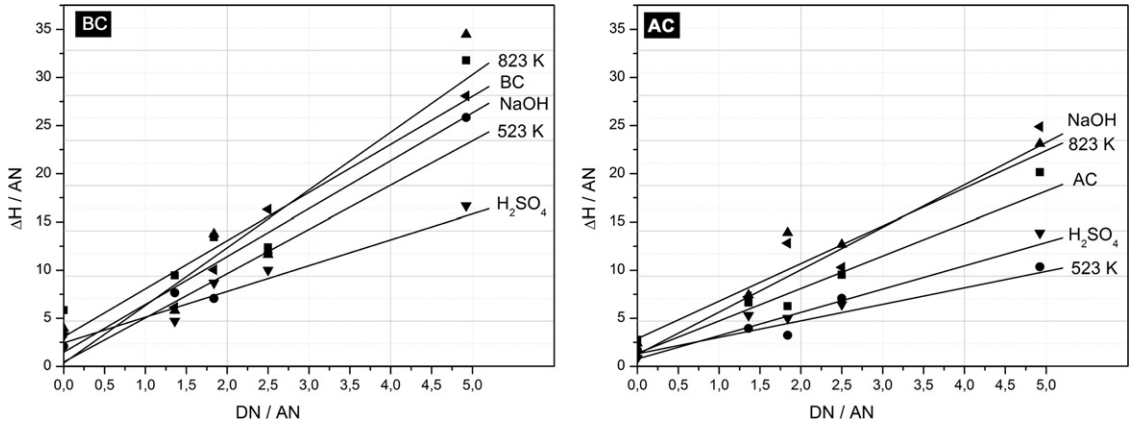

Fig. 6. Experimental determination of the acid–base properties for the natural and treated clays.

is plotted versus k_A the observed behaviour is an increase of the CEC with the acidity of the surface.

Finally, the morphological index I_M has been also calculated for the natural and treated clays. The results are also collected in Table 4. In accordance with the Brendle–Papirer method,[28] the negative values can be associated with surface nano-roughness and the more negative I_M values correspond to the roughest surfaces. I_M values between −5 and 0 are generally found for smooth surfaces, while layered silicates like H-magadiite, illites, etc., could give I_M values between −35 and −90.[38,42,43]

Results of Table 4 show that both smectites are rough materials being the BC sample the roughest one. When applying the heat treatment the nanoroughness of both clays decreases due either by the removing of water molecules and the increase in the pore size (Table 2). After H_2SO_4 and NaOH treatment, the I_M indexes decrease respect to those of natural clays, a result that also correspond to the destruction of the smectite clay structure. No correlation has been also found between I_M and CEC in this study.

4. Conclusions

In this study two natural smectite clays have been analyzed by different methods. These clays have then been thermal and chemical treated and also analyzed for comparing with natural ones. The main mineral components of both clays are smectite, quartz and kaolinite, and whereas BC clay contains calcite, it has been found illite structures into the AC clay. Moreover, quartz relative amount is higher in AC clay than in BC one. At moderate thermal treatment (523 K) the smectite structure remains unaltered for both clays while some water desorption occurs. Treating at higher temperature (823 K) leads to a collapse followed by dehydroxylation of layered sheets. At this temperature the structures of quartz, illite and kaolinite remain with some alteration. Chemical treatments with H_2SO_4 or NaOH also give a destruction of the smectite structure, with the elimination of calcite when present and dissolution of tetrahedrically coordinated Al and Si ions.

The surface adsorption and energy properties of these natural and treated clays have been also analyzed. BC clay presents higher CEC than AC clay, a result that can be due to its higher swelling property as it has observed by its higher water surface area. Pore sizes and porosities are very close for both materials and such surface properties vary in a similar form when they are thermal or chemical treated. The results obtained from the determination of the surface energy (dispersive and acid–base) indicate the similarity between the surfaces of the layers in both clays. The evolution of this surface property after any applied treatment follows a similar trend. However, from the I_M determination, it has been demonstrated that BC smectite presents higher nanorugosity than AC, a result that can be due to the higher quartz content of the AC clay. It is concluded that no correlation can be found between CEC and the surface energy or nanorugosity, however it has been observed an increase in the reduced CEC capacity with the acidity constant of both clays. This indicates that as the acid surface energy increases the CEC also does for a given surface area value.

Acknowledgements

Authors are grateful to the Ministerio de Educación y Ciencia of Spain for the financial support under the Project Ref. MAT2009-14450.

References

1. Vardoulakis E, Karamanis D, Assimakopoulos MN, Mihalakakou G. Solar cooling with aluminium pillared clays. *Solar Energy Mater Solar Cells* 2011;**95**(8):2363–70.
2. Patro TU, Wagner HD. Layer-by-layer assembled pva/laponite multilayer free-standing films and their mechanical and thermal properties. *Nanotechnology* 2011;**22**:45.
3. Zhuk A, Mirza R, Sukhishvili S. Multiresponsive clay-containing layer-by-layer films. *Acs Nano* 2011;**5**(11):8790–9.
4. Madejová J, Bujdak J, Janek M, Komadel P. Comparative ft-ir study of structural modifications during acid treatment of dioctahedral smectites and hectorite. *Spectrochi Acta A: Mol Biomol Spectrosc* 1998;**54**(10):1397–406.
5. Balard H, Saada A, Hartmann J, Aouadj O, Papirer E. Estimation of the surface energetic heterogeneity of fillers by inverse gas chromatography. *Macromol Symp* 1996;**108**:63–80.
6. Bhattacharyya KG, Sen Gupta S. Pb(ii) uptake by kaolinite and montmorillonite in aqueous medium: influence of acid activation of the clays. *Colloid Surf A-Physicochem Eng Asp* 2006;**277**(1–3):191–200.
7. Bhattacharyya KG, Sen Gupta S. Kaolinite, montmorillonite, and their modified derivatives as adsorbents for removal of cu(ii) from aqueous solution. *Sep Purif Technol* 2006;**50**(3):388–97.
8. Kheok S, Lim E. Mechanism of palm oil bleaching by montmorillonite clay activated at various acid concentrations. *J Am Oil Chem Soc* 1982;**59**(3):129–31.
9. Eren E, Afsin B. Investigation of a basic dye adsorption from aqueous solution onto raw and pre-treated sepiolite surfaces. *Dyes Pigments* 2007;**73**(2):162–7.
10. Benali S, Peeterbroeck S, Larrieu, me J, Laffineur F, Pireaux J-J, Alexandre M, et al. Study of interlayer spacing collapse during polymer/clay nanocomposite melt intercalation. *J Nanosci Nanotechnol* 2008;**8**(4):1707–13.
11. Bandosz TJ, Jagiello J, Andersen B, Schwarz JA. Inverse gas chromatography study of modified smectite surfaces. *Clays Clay Miner* 1992;**40**(3):306–10.
12. Cordeiro N, Silva J, Gomes C, Rocha F. Bentonite from porto santo island, madeira archipelago: Surface properties studied by inverse gas chromatography. *Clay Miner* 2010;**45**(1):77–86.
13. deCarvalho MB, Pires J, Carvalho AP. Characterisation of clays and aluminium pillared clays by adsorption of probe molecules. *Microporous Mater* 1996;**6**(2):65–77.
14. Saada A, Papirer E, Balard H, Siffert B. Determination of the surface properties of illites and kaolinites by inverse gas chromatography. *J Colloid Interface Sci* 1995;**175**(1):212–8.
15. Heller-Kallai L. Thermally modified clay minerals. In: Bergaya F, Theng BKG, Lagaly G, editors. *Developments in clay science*, vol. 1. 2006. p. 289–308. Chapter 7.2.
16. Stoch L, Bahranowski K, Budek L, Fijal J. Bleaching properties of non-bentonitic clay materials and their modification. *Mineral Pol* 1977;**8**(1):31–49.
17. Özcan AS, Özcan A. Adsorption of acid dyes from aqueous solutions onto acid-activated bentonite. *J Colloid Interface Sci* 2004;**276**(1):39–46.
18. Hisarli G. The effects of acid and alkali modification on the adsorption performance of fuller's earth for basic dye. *J Colloid Interface Sci* 2005;**281**(1):18–26.
19. Öztop B, Shahwan T. Modification of a montmorillonite–illite clay using alkaline hydrothermal treatment and its application for the removal of aqueous cs+ ions. *J Colloid Interface Sci* 2006;**295**(2):303–9.

20. Gregg SJ, Sing KSW. *Adsorption, surface area and porosity*; 1982. p. 303.
21. Kyziol-Komosinska J, Barba F, Callejas P, Rosik-Dulewska. C. Beidellite and other natural low-cost sorbents to remove chromium and cadmium from water and wastewater. *Bol Soc Esp Ceram Vidrio* 2010;**49**(2):121–8.
22. Wang JY, Charlet G. Use of moment analysis in inverse gas-chromatography. *Macromolecules* 1989;**22**(9):3781–8.
23. Dorris GM, Gray DG. Adsorption of n-alkanes at zero surface coverage on cellulose paper and wood fibers. *J Colloid Interface Sci* 1980;**77**(2):353–62.
24. Donnet J, Park S, Balard H. Evaluation of specific interactions of solid surfaces by inverse gas chromatography. *Chromatographia* 1991;**31**(9):434–40.
25. Saint Flour C, Papirer E. Gas-solid chromatography: a quick method of estimating surface free energy variations induced by the treatment of short glass fibers. *J Colloid Interface Sci* 1983;**91**(1):69–75.
26. Gutmann V. *The donor–acceptor approach to molecular interactions*; 1978. p. 279.
27. Riddle FL, Fowkes FM. Spectral shifts in acid–base chemistry. 1. Van der waals contributions to acceptor numbers. *J Am Chem Soc* 1990;**112**(9):3259–64.
28. Brendlé E, Papirer E. A new topological index for molecular probes used in inverse gas chromatography for the surface nanorugosity evaluation. *J Colloid Interface Sci* 1997;**194**(1):207–16.
29. Madejová J. Ftir techniques in clay mineral studies. *Vib Spectrosc* 2003;**31**(1):1–10.
30. Önal M, Sarikaya Y. Preparation and characterization of acid-activated bentonite powders. *Powder Technol* 2007;**172**(1):14–8.
31. Cases JM, Berend I, Besson G, Francois M, Uriot JP, Thomas F, et al. Mechanism of adsorption and desorption of water vapor by homoionic montmorillonite. 1. The sodium-exchanged form. *Langmuir* 1992;**8**(11):2730–9.
32. Breen C, Zahoor FD, MadejovÃ¡ J, Komadel P. Characterization and catalytic activity of acid-treated, size-fractionated smectites. *J Phys Chem B* 1997;**101**(27):5324–31.
33. Önal M, Sarıkaya Y. Thermal behavior of a bentonite. *J Thermal Anal Calorim* 2007;**90**(1):167–72.
34. Picard E, Gauthier H, J.F.Gérard, Espuche E. Influence of the intercalated cations on the surface energy of montmorillonites: consequences for the morphology and gas barrier properties of polyethylene/montmorillonites nanocomposites. *J Colloid Interface Sci* 2007;**307**(2):364–76.
35. Park SJ, Brendle M. London dispersive component of the surface free energy and surface enthalpy. *J Colloid Interface Sci* 1997;**188**(2):336–9.
36. Hamdi B, Kessaissia Z, Donnet JB, Wang TK. Variation de l'énergie superficielle d'une bentonite par traitement chimique et thermique. *Ann Chim Sci Matèr* 1999;**24**(1):63–73.
37. Slobodan MK. Surface properties of metal ions modified silicas. *Colloids Surf A: Physicochem Eng Aspects* 1999;**149**(1–3):461–6.
38. Ligner G, Vidal A, Balard H, n. Papirer E. London component of the surface energy of heat-treated silicas. *J Colloid Interface Sci* 1989;**133**(1):200–10.
39. Xie J, Bousmina M, Xu G, Kaliaguine S. Inverse gas chromatography studies of alkali cation exchanged x-zeolites. *J Mol Catal A: Chem* 1998;**135**(2):187–97.
40. Bilgic C, Tumsek F. Determination of the acid/base properties of mgy and nh4y molecular sieves by inverse gas chromatography. *J Chromatogr A* 2007;**1162**(1):83–9.
41. Bilgiç C, Topaloglu Yazıcı D, Vural N. Characterizing the surface acidity of bentonite by various methods. *Surf Interface Anal* 2010;**42**(6–7):1000–4.
42. Hadjar H, Balard H, Papirer E. An inverse gas chromatography study of crystalline and amorphous silicas. *Colloids Surf A: Physicochem Eng Aspects* 1995;**99**(1):45–51.
43. Comard M-P, Calvet R, Dodds JA, Balard H. Inverse gas chromatographic study of the surface properties of talc impregnated with different acidic and basic polymers. *Powder Technol* 2002;**128 2-3**:262–7.